

DIAGNOSTYKA, 2025, Vol. 26, No. 4

e-ISSN 2449-5220 **DOI:** 10.29354/diag/214933

THE USE OF WIRELESS VIBRATION SENSORS TO MONITOR THE TECHNICAL CONDITION OF INDUSTRIAL FANS

Kazimierz WITASZEK 1, * D, Łukasz DUSS 2 D

 Silesian University of Technology, Faculty of Transport and Aviation Engineering, Krasińskiego 8, 40-019 Katowice, Poland
 SOMAR S.A., ul. Karoliny 4, 40-186 Katowice, Poland
 *Corresponding author, e-mail: kazimierz.witaszek@polsl.pl

Abstract

The paper presents the practical application of a wireless vibration sensor system for the ongoing monitoring of the technical condition of industrial fans used in gas furnaces to heat metal billets prior to plastic working. During almost a year of research, vibration and temperature data was collected and subjected to time domain analysis. The measurement results were divided into weekly time intervals and statistically processed. In order to facilitate the decoding, segmentation into time-based segments, and statistical analysis of the research data, a software solution was developed. The application enabled the analysis of changes in weekly histograms and statistical parameters of data sets. A critical analysis was made of the statistical parameters obtained from the research material. The average weekly value of rms vibration acceleration and the highest weekly value of the relative frequency of data were selected as the parameters that best reflects changes in industrial fan technical condition. Functions modelling these changes were also developed. During the research, significant changes in the recorded vibration accelerations on fan motor No. 2 were observed. The developed functions proved useful for assessing and predicting changes in the technical condition of the tested fans.

Keywords: machine diagnostics, vibrations, wireless sensors, time domain analysis, vibration-based condition monitoring

List of Symbols/Acronyms

ARM – Advanced RISC Machines

avg, \bar{x} – average value of dataset;

CC0 - Creative Commons Zero 1.0 licence;

CDF – cumulative distribution function;

CF – crest factor;

 $csv-comma-separated\ values\ file;$

DF – dynamic factor;

 $f_1(t), f_2(t), f_3(t), f_4(t)$ – declared functions;

FFT – Fast Fourier Transform algorithm;

GPRS - General Packet Radio Service;

Havg - average relative frequency of data;

H_{max} – highest relative frequency of data;

i – measurement index;

IT – Information Technology;

 $kurt,\,\gamma_2-kurtosis;$

max, peak - maximum, largest observation;

med, Q2 - median;

MEMS – micro-electromechanical systems;

mod – mode, dominant;

n – number of recorded measurements;

nw – number of measurements during week;

 $Q_1-first\ quartile;$

Q₃ – third quartile;

R – Pearson correlation coefficient;

 R^2 – coefficient of determination;

RMS – effective value (Root Mean Square);

std, σ – standard deviation;

Temp. – temperature;

VCBM - vibration-based condition monitoring

1. INTRODUCTION

Machines and equipment used in metallurgical plants often operate in very harsh environmental conditions. High loads, continuous operation and dust often affect their technical condition. An unforeseen failure of such equipment can even lead to a production line stoppage, which results in significant material losses for the company. That is why systems are being developed and implemented to monitor the technical condition of companies' machinery [1 - 3].

A properly designed system for monitoring the technical condition of machinery measures selected physical quantities, and the measurement results are collected and analysed on an ongoing basis [4, 5]. Various physical quantities that are measurable and correlate with the progressive wear or degradation of the functional properties of the monitored machine can be used as parameters for assessing the technical condition [6]. Systems are used to monitor the temperature of bearing nodes, working parts and machine engines. A rise in temperature may indicate

Received 2025-11-10; Accepted 2025-12-01; Available online 2025-12-03

^{© 2025} by the Authors. Licensee Polish Society of Technical Diagnostics (Warsaw. Poland). This article is an open access article distributed under the terms and conditions of the Creative Commons Attribution (CC BY) license (http://creativecommons.org/licenses/by/4.0/).

a deterioration in lubrication conditions or overload. Even inexpensive technical devices, such as power tools, are often equipped with thermal switches that disconnect the motor when the safe operating temperature range is exceeded. Most of the drives of machines operating in industrial plants are based on electric motors. Therefore, the results of measuring the current consumed by the motor can be used as a diagnostic parameter. This is all the more so as motors are increasingly working with controllers (e.g. inverters) that have built-in current measurement circuits. A deterioration in technical condition can increase movement resistance, which will be detected by the system as an increase in the machine drive's electricity demand.

One of the most commonly used methods in industrial practice is vibroacoustic diagnostics of technical objects or vibration-based condition monitoring (VBCM) [7]. Many papers have been published describing the application of vibroacoustic methods in the automotive industry [8 - 10] or, more broadly, in transport [11, 12], as well as in the diagnostics of industrial machinery and equipment [13 - 15].

When used correctly, it allows for early detection of symptoms of impending machine failure. The key to the effective use of vibroacoustic methods is the correct selection of signal processing methods. The analysis may consist of comparing current measurement results with predefined threshold values, or more advanced computational methods tracking trends, such as time domain analysis, may be used [16, 17]. By examining data that changes over time, it allows for the identification of trends in the measured quantities. This method is one of the less complicated ones and is therefore widely used in practice in a variety of applications [18, 19]. It involves collecting measurement data from a vibration sensor, eg. vibration acceleration [20] and then calculating statistical parameters describing the collected data. Changes in the values of selected parameters over time should correlate with changes in the technical condition of the machine under test.

A frequently selected statistical parameter of the signal is its effective value (RMS) [21 - 23], expressed by formula 1.

$$RMS = \sqrt{\frac{\sum_{i=1}^{n} x_i^2}{n}} \tag{1}$$

where:

i – measurement index,

n – number of recorded measurements,

 x_i – value of a specific measurement.

According to the results of [24], a change in the effective value allows for the detection of, in particular, the imbalance of rotating machine parts. However, it may not be sensitive enough to detect early signs of failure.

Another statistical signal parameter frequently used in practice is the peak value of the recorded vibrations [23]. It is calculated according to formula 2.

$$peak = |v(t)| max.$$
 (2)

where:

v(t) – measured signal

As the damage progresses, the peak values of the forces exerted by the rotating elements also increase. However, it should be noted that despite the advantages associated with the simplicity of the algorithm for determining maximum values, this parameter is sensitive to noise and random events occurring in the measurement system.

Based on the two parameters described above, a quantity called the peak factor can be created [21, 23], described by formula 3.

$$CF = \frac{peak}{RMS} \tag{3}$$

Due to its independence from rotational speed, this parameter is useful in cases of monitoring devices operating at variable rotational speeds. However, there are areas where its usefulness is limited, e.g. bearing diagnostics.

A more computationally complex statistical parameter of a data set is kurtosis [23], described by formula 4.

$$kurt = \gamma_2 = \frac{\mu_4}{\sigma^4} = \frac{\frac{1}{n} \sum_{i=1}^{n} (x_i - \bar{x})^4}{\left(\frac{1}{n} \sum_{i=1}^{n} (x_i - \bar{x})^2\right)^2}$$
(4)

where:

μ₄ – fourth central moment,

 σ – standard deviation,

 \bar{x} – average value of measurements.

It is a dimensionless quantity describing the distribution of the measured quantity. Its advantage is that it is not sensitive to changes in load or rotational speed. Kurtosis analysis is sometimes used competitively with the peak factor, but the latter is more widely used in practice.

In more advanced cases, frequency domain analysis methods are used [25, 26] for example FFT [27] or wavelet approach [28]. Vibration-based condition monitoring systems also frequently employ sophisticated computational methodologies, including neural networks [29], deep machine learning [30, 31], and fuzzy logic [32].

Breaking down the measured signal into its component frequencies allows for a broader analysis and detection of faults manifested by changes in limited frequency ranges [33]. Although the computational complexity of, for example, FFT analysis is much greater than that of the time domain analysis methods discussed above, the increase in the computing power of IT systems and microcontrollers available on the market allows the use of preprocessing algorithms already at the first stage of data acquisition. Modern sensors are most often equipped with digital outputs that work with a microcontroller built into the sensor. The dynamic development of 32-bit microcontrollers based on the ARM core, which currently have significant computing power and memory resources, has significantly influenced the design philosophy of measuring devices [7, 34]. In contrast to classic 8-bit solutions, it is now possible to use advanced signal processing at the sensor stage, such as performing FFT analysis.

The evolution of electronic, wireless data transmission systems has had a significant impact on the design and construction of vibroacoustic diagnostic systems [35]. The utilisation of solutions that do not necessitate the use of cables for both power supply and data transmission is gaining popularity. The utilisation of such solutions is particularly advantageous when the measurement of machines already in operation within industrial contexts is required. In such cases, there is no necessity to modify the existing cabling infrastructure. Wireless sensors are most often powered by chemical energy sources. The development of solutions that are based on the acquisition of diverse forms of energy and its subsequent conversion to electricity is also underway. This process is referred to as energy harvesting [36]. The utilisation of such solutions enables the construction of self-powered sensors that do not require periodic replacement or recharging of power sources.

2. MEASURING SYSTEM

The tests were conducted using the SDM-1 machine diagnostics system developed and implemented by the Katowice-based company Somar S.A. in one of the non-ferrous metal processing plants in central Poland as part of the project 'Hardware and software system for the diagnostics of machines and devices based on a wireless network of monitoring sensors and methods of knowledge engineering and computational intelligence'. During the work, the technical condition of machines crucial for the continuity of the plant's production process was monitored, such as fume extraction fans, gas furnace fans, 42 MPa pumps, 60 MPa pumps, emulsion filtration pumps, conveyor rollers and coiler drive gears.

WS-VT1 sensors were placed in selected locations on the devices to measure vibrations and temperature at these points. WS-VT1 sensors (Fig. 1) are advanced devices based on a microcontroller that works with, among other things, a three-axis MEMS accelerometer, a semiconductor temperature measurement circuit and an 868 MHz transceiver. These sensors are completely wireless in terms of both power supply and data transmission, so they do not require any cabling of the tested devices. This is particularly important in the case of industrial machines that are already in operation.

The WS-VT1 sensor is powered by a built-in LS 14250 lithium battery, which, thanks to the use of hardware solutions and energy-saving algorithms, can power the sensor for up to several months. The length of the operating period between battery replacements depends on the sensor's operating parameters, mainly the frequency of measurements and data transmission. During the measurement cycle, the built-in triaxial MEMS accelerometer

performs a series of measurements, the results of which are processed by a microcontroller. The results are given as the effective value of vibration acceleration (vibr AVG) and the maximum value of recorded vibrations (vibr MAX). These values, supplemented by temperature measurement results and diagnostic parameters such as the sensor's battery voltage and radio signal level, are sent to the diagnostic system's transceivers. When employing a vibration sensor, consideration should be given to its mounting [37]. The sensor can be mounted on the tested device in a non-invasive manner by gluing or using a magnetic adapter. It is also possible to use an M12 threaded connection. The method of connecting the sensor has little effect on its frequency characteristics (Fig. 2).



Fig. 1. Somar WS-VT1 vibration and temperature sensor

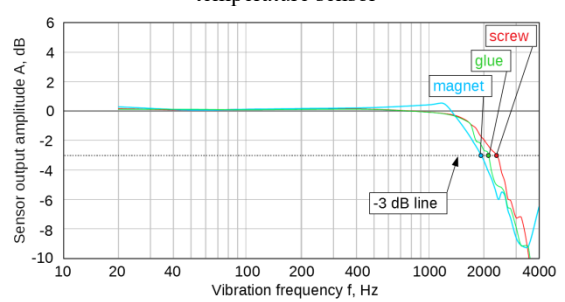


Fig. 2. Frequency response of the WS-VT1 sensor

The onboard microcontroller collects measurement results, pre-processes them and sends data frames to the ITR-2 transceiver using the 898 MHz band. One transceiver can support multiple sensors, both reading data from them and sending messages controlling their operation. The transceiver communicates with its surroundings via a mobile network using GPRS technology. Data can be collected on a local server or, as in the case of the implemented solution, via an Internet connection and using the server infrastructure of the monitoring service provider. Such cloud type server [38] provides the functionality of a typical database enriched with an analytical and visualisation layer. A convenient option is the built-in visualisation interface accessible via a website for devices at the customer's location. The basic diagram of the implemented SDM-1 system, from which the research data was obtained, is shown in Figure 3.

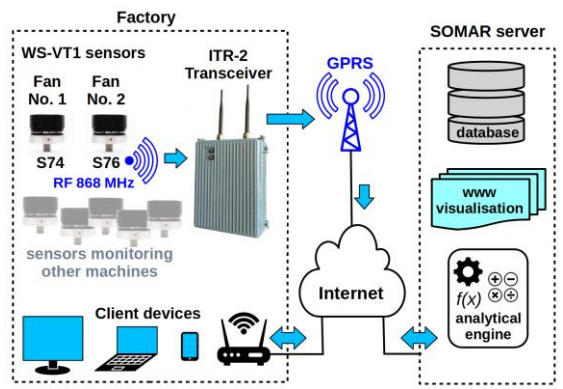


Fig. 3. Diagram of the SDM-1 system used in the research

The study analysed data obtained from sensors installed on gas furnaces fan motors used to heat billets before rolling. The rotors of these fans are driven by asynchronous three-phase motors with a rated speed of 2940 rpm. The first of the tested fans (No. 1) used a 37 kW motor weighing 255 kg. A WS-VT1 sensor marked S74 (Fig. 4) was installed on the front part of the motor body, which transmitted information about the vibrations and temperature of the tested device.

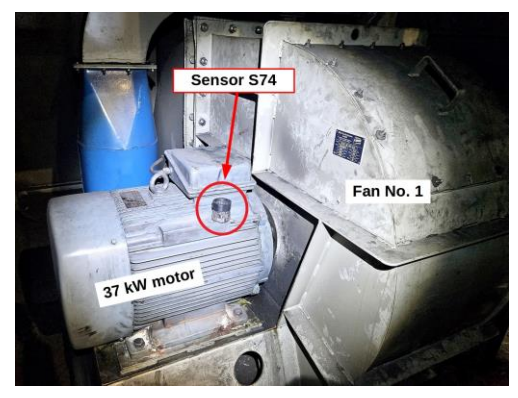


Fig. 4. Gas furnace fan No. 1

The second of the tested fans (No. 2) was driven by a 45 kW motor weighing 353 kg. A sensor marked S76 was installed on the front cover of the motor (Fig. 6). The selected sensor locations enabled monitoring of the motor's operation and the technical condition of its shaft bearings.

3. RESEARCH RESULTS

The research data reflects less than a year of operation of the tested devices in a metallurgical plant. It comes from the SDM-1 system database for the period from 23 October 2024 to 11 August 2025 for sensor S74 (292 days). The data for sensor S76 covers the period from 7 November 2024 to 7 October 2025 (335 days). The data was transmitted and stored on the diagnostic monitoring service provider's server at default intervals of 10 seconds. An extract was made from the database to *.csv text files. In line with supporting policies that promote open access to data, files containing raw

measurement data have been uploaded to the RepOD open database and made available under a Creative Commons Zero 1.0 licence (CC0) [39].



Fig. 5. Gas furnace fan No. 2

The first line is the header, and the remaining lines contain the test data. Each line is a single data record containing information about the date and time of the measurement and, separated by semicolons, the measured temperature, maximum vibration acceleration and effective vibration acceleration values (Fig. 6). During the extraction, auxiliary diagnostic data such as sensor battery voltage and radio signal strength were omitted.

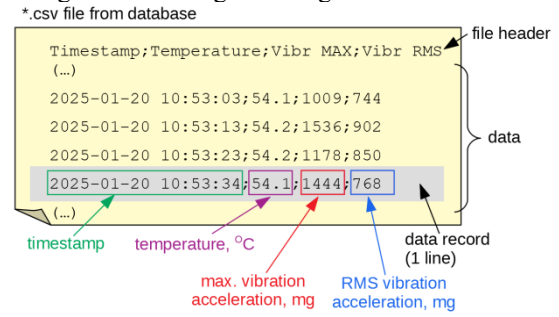


Fig. 6. Structure of research data contained in the *.csv file

During the study period, approximately 8,640 measurement records were collected per day, which, when converted to the length of the study period, gives over 2.5–2.8 million measurement records for each of the sensors included in the study.

The results obtained are presented graphically in the charts (Fig. 7 and 8).

The values recorded during the measurements are presented as small dots without connecting them with lines. This allows for a preliminary assessment of the areas of concentration of the results. However, the figures show a significant spread of measurement results, which makes it difficult to draw conclusions based on raw measurement data. Due to the very large number of recorded results, the points on the graph merge into coloured areas.

4. ANALYSIS OF RESEARCH RESULTS

In order to carry out the application process correctly, it is necessary to process the research data. The data package size is 85 MB for the S74 sensor

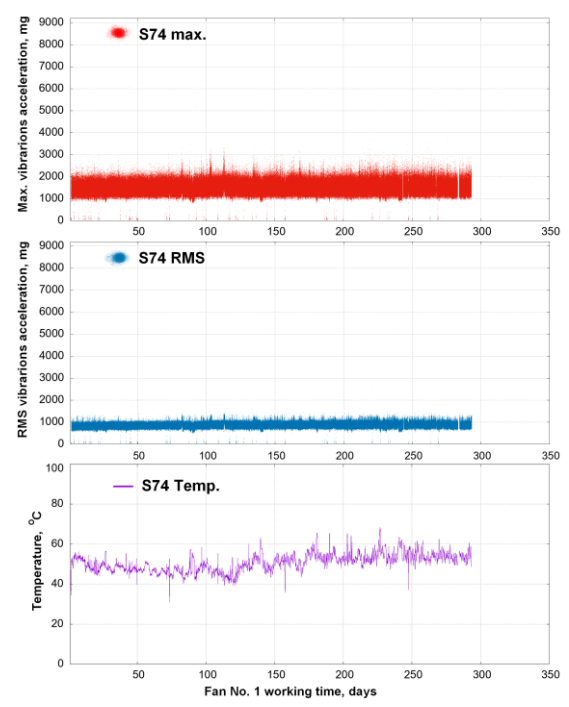


Fig. 7. Data from sensor C74

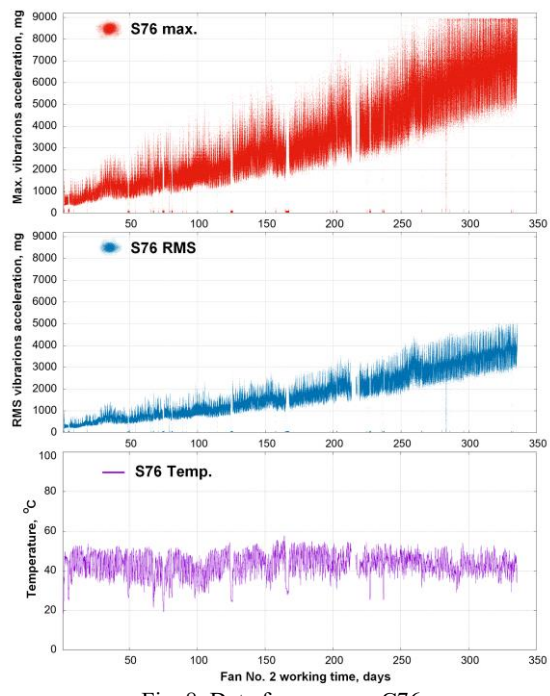


Fig. 8. Data from sensor C76

and 95 MB for the S76 sensor. With such large files, it is practically impossible to process them in popular spreadsheet programmes. Therefore, in order to perform calculations efficiently, the VIBRCALC software was written in Pascal and compiled into an executable file for Windows (WIBRCALC.exe) using the publicly available Free Pascal v.3.2.2 compiler. Due to the functional nature of the programme and the possibility of running it in the background, no graphical interface was designed, and it was decided to operate the programme in command line mode. Additionally, this allows for batch mode operation with minimal user interaction,

which is limited to specifying the programme's operating parameters. The VIBRCALC programme's operating algorithm is shown in Figure 9. The parameters controlling the programme's operation are specified when it is called in the command line. They are listed in Table 1.

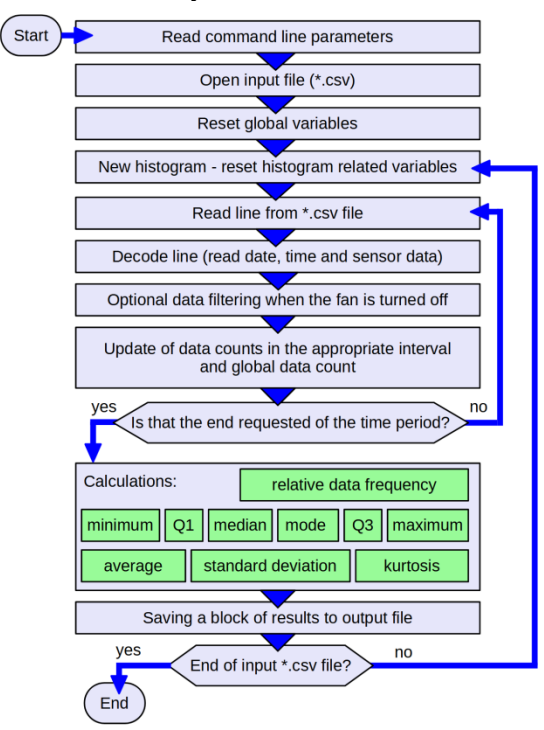


Fig. 9. VIBRCALC programme operation algorithm

Thanks to the universal design and parameterisation of the programme, it is possible to perform calculations for histograms, determine average values, standard deviations, medians or other statistical parameters for the entire data set as well as for virtually any specified time intervals. This allows to create histograms showing changes in data distribution over successive time intervals.

Table 1. VIBCALC programme start-up parameters

P-	-8
Parameter	Format
File name	<file name="">.csv</file>
Number of histogram	1 1000
data intervals	
Maximum histogram	0,1 - 10000
value range	
Data selection from the	1 – Temperature
sensor	2 – Vibr MAX
	3 – Vibr RMS
	4 – Peak factor
	(calculated)
The time range for	0.1 30000 h
calculating histogram	
components	
Data filter for a switched-	0 8000 mg for vibr RMS
off machine, cutting off	
results below a specified	
value	

The programme works in a loop, sequentially reading lines of data from the input *.csv file. Then, using information about the data format, it decodes them from text to numerical form stored in the computer's memory. It then performs the necessary calculations cyclically and, when the end of the time interval is reached, saves the partial results to a text file containing the results of the work.

Firstly, the frequency of data occurrence in specified value intervals was calculated. Based on this, histograms were created for the entire data sets. The width of the intervals was set at 25 mg. The vibration acceleration histogram for the S74 sensor is shown in Figure 10.

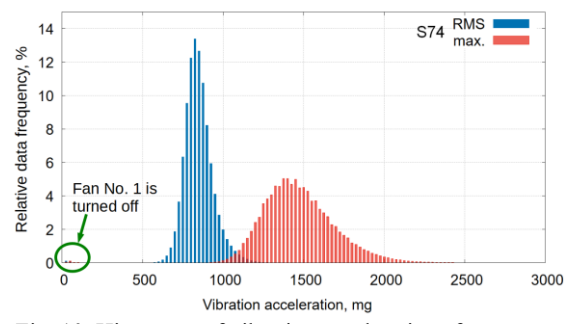


Fig. 10. Histogram of vibration accelerations from sensor S74

The histograms of recorded vibration accelerations for sensor S74, both for maximum and RMS values, have two local maxima. The first one is on the left side of the graph and is barely noticeable. It corresponds to the recorded background vibrations when the fan motor is switched off. The vibration acceleration values are then less than 100 mg. There is a clear break, and only at values above several hundred mg can the main part of the histograms be seen. For RMS values, the histogram is quite narrow, as most of the results are in the range of 500-1400 mg. There is a clear dominance in the range of 825 mg, with as much as 13.4% of the results falling within this range. The data distribution is slightly asymmetrical towards higher acceleration values.

The histogram of the maximum vibration measurement results is shown in Figure 10 using red. It is shifted towards higher vibration acceleration values. The results are mainly in the range of 800–2500 mg. It is less slender than the one described previously and does not have a very clear dominant. The highest frequencies were recorded in the vibration acceleration ranges of 1375, 1400 and 1450 mg, respectively, and account for approximately 5% of the results. A slight asymmetry of the distribution towards higher vibration acceleration values is also more noticeable.

A vibration acceleration histogram was also developed for the S76 sensor, as shown in Figure 11.

For both maximum and RMS vibration accelerations, the histograms are clearly flattened and contain numerous local maxima. This is due to the gradual increase in vibrations during the test

period, which was visible in Figure 8 showing the raw data from the sensor. As before, it is possible to distinguish the background vibration area when fan #2 was not operating. These are ranges below 125 mg for effective values and below 250 mg for maximum vibration acceleration values.

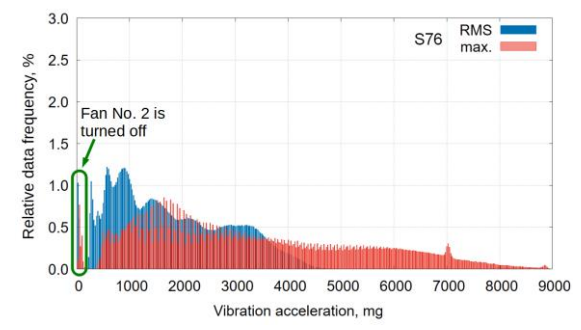


Fig. 11 Histogram of vibration accelerations from sensor S76

The data range for the operating fan is between approx. 200 - 4950 mg for the recorded effective values and 375 - 8950 mg for the series of maximum values. Both distributions shown in Figure 11 are asymmetrical. As with the S74 sensor, the dominant value is clearly on the left side of the graph, and the right side of the distribution is elongated.

Histograms were created in a similar manner for the temperatures recorded during the operation of the tested fans (Fig. 12). The distributions of recorded temperatures are similar, but they are shifted relative to each other by less than 10°C. The data indicate that the S74 sensor recorded slightly higher temperatures.

Based on the collected research data on vibration acceleration values, cumulative distribution functions were developed and compiled in Figure 13. This figure also includes information on the mean values, Q2 median, Q1 and Q3 quartiles, and modes (dominants). The curves in Figure 13, like the previously presented histograms, reflect the general characteristics of the research data sets. The large angle of inclination of the curve in its middle section corresponds to a narrow histogram, as is the case with data from sensor S74.

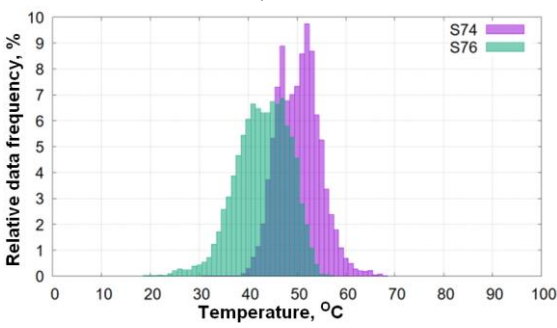


Fig. 12. Comparison of temperature histograms recorded during research

The cumulative distributions for data obtained from sensor S76 show significantly smaller angles of inclination, which corresponds to wide and flat histograms. Figure 13 clearly shows the asymmetry of the data distribution. All dominants are below the median, while the mean values are above the median.

Next, the data was analysed in time intervals. Due to the long data collection period, it was decided to perform calculations covering data from a week. The use of relatively long time intervals resulted in a reduction in the dispersion of results. This was evident when compared to the results of preliminary analyses conducted in daily intervals.

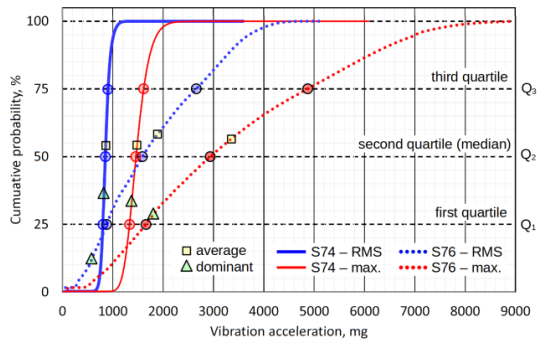


Fig. 13. Comparison of cumulative distribution functions (CDF), average values and dominant vibration accelerations based on collected test results

For each 7-day time interval, slightly over 60,000 data records were accepted. The VIBRCALC programme divided the data into individual series based on the value of the decoded time stamp. All recorded results were included in the current range, from 00:00:00 on the first day to 23:59:59 on the seventh day. If the fan operated for less than 168 hours in a given week, the amount of data included in the calculations was less than initially assumed. Only data collected during fan operation was taken into account. Thanks to this, data from the period when the tested device was switched off did not affect, for example, the underestimation of the weekly average value. Therefore, the data filtering option in the VIBRCALC programme was enabled. Based on the information obtained when creating histograms and CDFs, it was decided that all measurement records in which the recorded results of the Vibr RMS variable are less than 125 mg will be filtered.

Changes in the distribution of data in subsequent measurement weeks can be observed in threedimensional histograms. These are sets of connected two-dimensional histograms calculated for each subsequent week of testing. The height of the point above the xy plane corresponds to the relative frequency of vibrations. To improve the readability of the graphs, a colour scale corresponding to the results on the graph axis has been added. In order to show the variability of the data over the course of successive weeks of testing as accurately as possible, the figures have been supplemented with generated 2D maps of the weekly distribution of maximum and RMS vibration accelerations. The data for sensor S74 is shown in Figure 14, while the data for sensor S76 is shown in Figure 15.

For both analysed fans, changes in the distribution of vibration accelerations can be

observed during the research. Over time, the height of the histogram decreases and its base width increases. Additionally, it can be observed that the range of data recorded in subsequent days shifts towards higher vibration acceleration values.

For the S74 sensor, these changes are minor but noticeable. After almost 50 weeks of testing, the height of the histograms of the weekly distribution of the RMS vibration value decreases by about 20%. The range of recorded data shifts slightly but noticeably, with the RMS value of vibration acceleration increasing by about 15%.

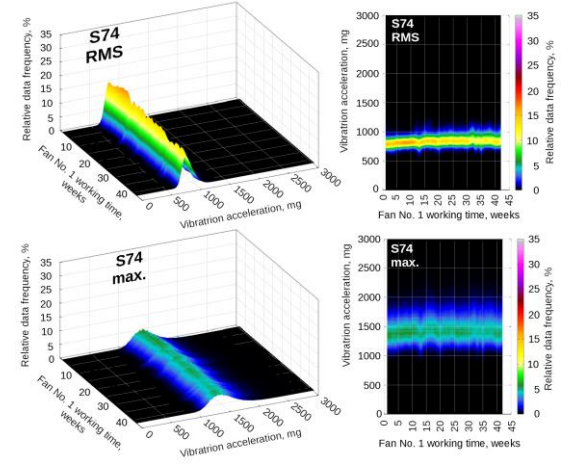


Fig. 14. Weekly changes in the distribution of vibration accelerations recorded by sensor S74

For the data obtained from the S76 sensor, the variability of the weekly data distributions is very clear (Fig. 15).

During the period under study, there was a several-fold increase in the recorded vibration accelerations. On two-dimensional maps, it can be assessed that the trend of these changes is progressive. At the same time, the height of the histogram decreases several times and its base width increases, which indicates a progressive degradation of the technical condition of the fan monitored by the S76 sensor.

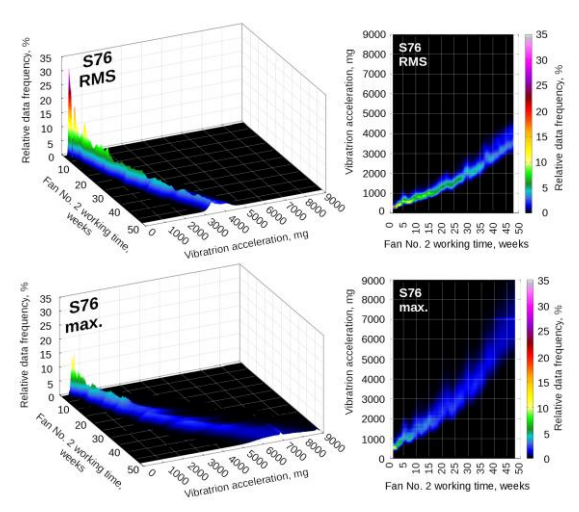


Fig. 15. Weekly changes in the distribution of vibration accelerations recorded by sensor S76

Due to the data acquisition algorithms built into the sensor, there may be a mutual correlation between the maximum and RMS vibration acceleration values stored in the database. This is because the sensor takes a series of measurements and stores the results in its internal memory, then uses this set to determine the RMS and maximum values. The correlation between these waveforms can also be inferred from Figures 7, 8, 14 and 15. Therefore, the raw vibration acceleration data (Fig. 16a) and their weekly averages (Fig. 16b) are shown in the graphs. Weekly averages were calculated from formula 5. The squares of the correlation coefficients were also calculated.

$$avg = \frac{\sum_{i=1}^{n_W} x_i}{n_W} \tag{5}$$

where:

 n_w – number of measurements during week.

For data from sensor S74 monitoring the condition of fan No. 1, there is some correlation, but due to the relatively small range of changes in the observed vibrations for the raw data, it is not strong (R^2 =0.423). Although the weekly averages from the measurements show a higher correlation (R^2 =0.78), the range of variation in the results is very small. Both on the x and y axes, it is no more than 200 mg.

The data from fan No. 2 collected by sensor S76 show high dynamics. Initially, slight vibrations were observed, which increased to the upper measurement range of the sensor during almost a year of testing. Hence, Figure 16 shows a clearly diagonal cluster of data. This indicates a clear correlation between the effective and maximum vibration acceleration values. For raw measurement results, the correlation coefficient square is (R²=0.856). For weekly averages, the correlation is very strong (R²=0,998).

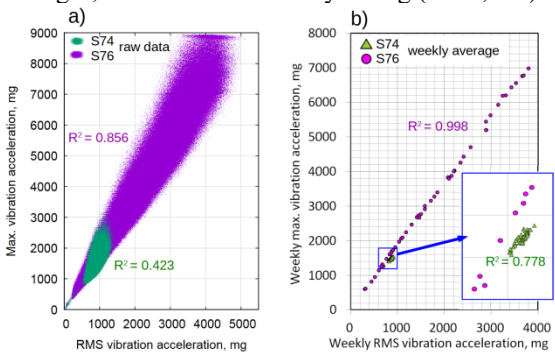


Fig. 16. Mutual correlation between maximum and RMS values of vibration acceleration

In order to check whether other data collected during the tests change their weekly values over time, the recorded temperature values and the peak coefficient for vibration accelerations were taken into account.

Next, a correlation matrix was calculated for the available weekly average values (Fig. 17). Additionally, the matrices were supplemented with dynamic factor (DF) which is rate of change indicator calculated using formula 6. It is the ratio of the weekly average values of a given quantity from the last week of the study to that from the first week.

$$DF = \frac{avg(last week)}{avg(first week)} \tag{6}$$

This parameter helps to assess whether the set of results has changed significantly during the tests.

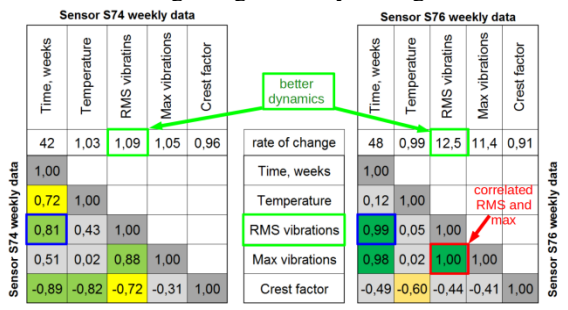


Fig. 17. Mutual correlation between maximum and effective values of vibration acceleration

Figure 17 shows that it is much easier to identify test data for fan No. 2 that is significantly correlated with time, as the data from sensor S76 is characterised by significant dynamics of changes in vibration acceleration. In addition, there is a strong correlation between their weekly effective and maximum values. For fan No. 1, the appropriate diagnostic parameter can be selected by taking into account both the results of the correlation matrix and the dynamics of changes. In general, it can be noted that the changes in average temperatures and the calculated peak coefficient recorded during the tests are insignificant, and therefore it is not justified to draw conclusions about the technical condition of the fans on this basis. The maximum weekly value of vibration acceleration for sensor S74 shows a weak correlation with the test time, and for sensor S76 it can be ignored due to its strong correlation with the RMS value. Therefore, the results of the measurements of the RMS value of vibration acceleration recorded by sensors S74 and S76 were taken into account.

Based on weekly data sets with an average of approximately 60,000 RMS vibration acceleration values, many statistical parameters describing them can be determined. In addition to the mean (avg) and standard deviation (std), these are read from the distribution as follows:

- minimum value (min),
- first quartile (Q1),
- median (med),
- third quartile (Q3),
- maximum value (max).

Additionally, for weekly histograms, the following were determined:

- kurtosis (kurt),
- mode, dominant (mod),
- highest relative frequency of data (H_{max}),
- average relative frequency of data (H_{avg})

In order to assess the usefulness of these parameters for evaluating changes in the technical condition of fans, correlation matrices [40] were created, which are shown in Figures 18 and 19.

S74 RMS	week	avg	std	min	Q1	med	Q3	max	kurt	mod	H _{max}	H _{avg}
week	1,00		possible correlation of data with operating time									
avg	0,81	1,00										
std	0,68	0,68	1,00			р	ossib	le cro	OSS C	orrela	ation	
min	0,25	0,19	0,07	1,00			ı	of	data			
Q1	0,72	0,96	0,47	0,17	1,00							
med	0,81	0,99	0,64	0,17	0,97	1,00						
Q3	0,85	0,99	0,75	0,17	0,91	0,98	1,00					
max	-0,19	-0,07	-0,09	-0,26	-0,05	-0,07	-0,08	1,00				
kurt	-0,27	-0,23	-0,29	-0,22	-0,17	-0,23	-0,26	0,83	1,00			
mod	0,66	0,87	0,47	0,12	0,90	0,89	0,83	-0,13	-0,29	1,00		
H _{max}	-0,77	-0,68	-0,94	-0,11	-0,48	-0,67	-0,78	0,15	0,34	-0,50	1,00	
Havg	0,07	0,01	-0,24	0,82	0,06	0,01	-0,02	-0,33	-0,23	0,03	0,17	1,00

Fig. 18. Correlation matrix of statistical parameters of weekly effective acceleration values from sensor S74

The data shown in the first column indicates that the mean, median and third quartile show the highest correlation with the passage of weeks for sensor S74. At the same time, all these variables are strongly correlated with each other, so they form a single group. A relatively high negative correlation with the passage of time is shown by the data series containing the calculation results for the highest relative frequency of data (H_{max}), so it may be another parameter showing changes in the technical condition of the device over time.

Two data groups can also be found for sensor S76. The first strongly correlated group consists of the mean, standard deviation and most of the data read from the cumulative distribution function (Q1, med, Q3, max) and the dominant. They illustrate the increase in vibration levels over time. The second mutually correlated group consists of values related to the height of the histogram bars (H_{max} i A_{avg}). Their values decrease over time and show a reduction in height and a widening of the histogram base.

ouse	ouse.											
S76 RMS	week	avg	std	min	Q1	med	Q3	max	kurt	mod	H _{max}	H _{avg}
week	1,00		possible correlation of data with operating time									
avg	0,99	1,00										
std	0,96	0,97	1,00			р	ossib	le cro	SS CO	ı orrela	tion	
min	0,63	0,64	0,64	1,00					data			
Q1	0,99	1,00	0,97	0,64	1,00							
med	0,99	1,00	0,97	0,64	1,00	1,00						
Q3	0,98	1,00	0,97	0,64	1,00	1,00	1,00					
max	0,97	0,98	0,95	0,62	0,98	0,98	0,97	1,00				
kurt	-0,29	-0,26	-0,30	-0,17	-0,26	-0,26	-0,26	-0,10	1,00			
mod	0,99	1,00	0,97	0,63	1,00	1,00	1,00	0,98	-0,26	1,00		
H _{max}	-0,74	-0,69	-0,74	-0,45	-0,68	-0,69	-0,69	-0,63	0,70	-0,69	1,00	
Havg	-0,84	-0,79	-0,83	-0,44	-0,79	-0,79	-0,79	-0,83	0,27	-0,80	0,84	1,00

Fig. 19. Correlation matrix of statistical parameters of weekly effective acceleration values from sensor S76

Based on the analysis of data from Figures 18 and 19, two parameters common to both tested fans were selected for further analysis: the average weekly effective value of vibration acceleration and the highest weekly value of relative data frequency (H_{max}) i.e. the height of the histogram bar for the

dominant frequency. Based on these parameters, functions describing changes in the technical condition of the fans during the tests were determined. Gnuplot 5.4.8 software was used to determine the form of the functions [41], which allows the parameters of a user-defined function to be determined using the Levenberg-Marquardt nonlinear algorithm.

After a preliminary analysis of the results for modelling data from the S74 sensor, due to the significant dispersion of the results, linear functions defined by formulas 7 and 8 were selected

$$f_1(t) = a_1 t + b_1 (7)$$

$$f_2(t) = a_2 t + b_2 (8)$$

A second-degree polynomial defined by the formula 9 was selected as the function modelling the average weekly effective values of vibration acceleration.

$$f_3(t) = a_3 t^2 + b_3 t + c_3 \tag{9}$$

However, the decrease in the weekly histogram of the effective acceleration value during the tests is best reflected by the power function defined by the formula 10.

$$f_4(t) = a_4 t^{-b_4} (10)$$

The Gnuplot programme performed cyclical calculations, selecting the values of the parameters a_i , b_i , c_i and calculating the standard asymptotic error for each of the determined parameters, which allowed for a reliable assessment of the selection of functions for the data set. The results of the selection of function parameters are presented in Table 2.

In the case of fan No. 1, the results of the selection of function parameters describing changes in the weekly average values of vibration accelerations recorded by the S74 sensor show noticeable uncertainty, which is confirmed by the relatively low values of the R² correlation coefficient. This is caused by the small range of changes in the technical condition of fan No. 1 during the tests and measurement noise.

Table 2. Results of function parameter selection

function	Parameter		Error, %	Function to data R ²		
C (1)	a_I	1,742	11,31	0,662		
$f_1(t)$	b_I	823,0	0,59	0,002		
$f_2(t)$	a_2	-0,001	12,96	0.500		
	<i>b</i> ₂	0,162	2,16	0,598		
f3(t)	a_3	0,879	7,49			
	<i>b</i> ₃	30,25	11	0,997		
	C3	375,8	9,41			
f4(t)	<i>a</i> ₄	0,321	3,29	0,972		
	b_4	-0,568	3,03	0,972		

However, for fan No. 2 monitored by sensor S76, changes in technical condition are clearly visible even in the raw data set. Therefore, the selected functions $f_3(t)$ and $f_4(t)$ describing the relationship between the average weekly effective value of

vibration accelerations and the change in the highest relative frequency of data since the fan's operation show a very high correlation with the research data sets, as the calculated correlation coefficient square is as high as 0,997 for $f_3(t)$ and 0,972 for $f_4(t)$.

The values of previously selected weekly data and functions reflecting changes in the technical condition of fan No. 1 are shown in Figure 20. They show a slight increase in the average weekly RMS vibration values recorded by sensor S74 (Fig. 20a).

A decrease in the height of the histogram is also observed, which is consistent with the changes observed in Figure 14. However, there is a significant spread of results, which reduces the correlation coefficient.

Changes in the technical condition of fan No. 2 and functions describing weekly data are shown in Figure 21. Despite the small spread of results, the functions are selected with a high degree of certainty, and the obtained relationships correspond to the observations described for the 3D histogram shown in Figure 15.

For fan No. 2, the selection of functions was additionally verified by comparing the prediction for a period of 4 weeks with subsequent data downloaded from the system.

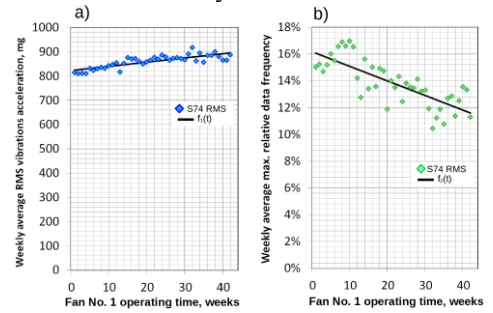


Fig. 20. Data and functions reflecting changes in the technical condition of fan #1

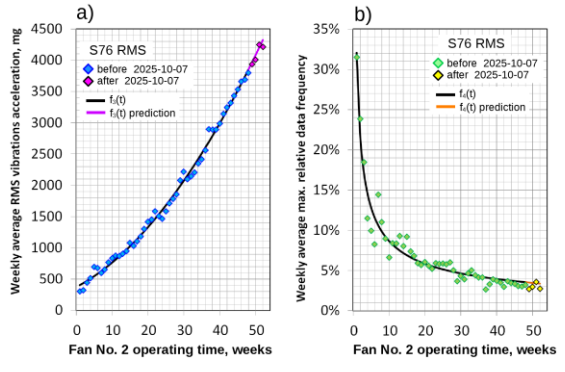


Fig. 21. Data and functions reflecting changes in the technical condition of fan #2 and a 4-week forecast

For the $f_3(t)$ function, the forecast of the average weekly RMS vibration values coincided with the obtained points. For the $f_4(t)$ function, the forecast lies within the range of measured values, but there is a greater spread of results. For diagnostic purposes, the $f_3(t)$, function is more useful, and its estimated computational complexity even allows for its implementation in a microcontroller controlling the

operation of WS-VT1 sensors during further development work.

5. CONCLUSIONS

The results of the research conducted in this study demonstrate the advantages of using a long-term monitoring system for the technical condition of industrial machinery and equipment.

The implementation of a system utilising wireless sensors to monitor the technical condition of machinery and equipment in a heavy industrial plant has demonstrated the effectiveness of such a solution. The installation of the sensors was not technically problematic, and the radio signal strength was sufficient to obtain accurate readings. However, it should be noted that a potential drawback associated with this system is the periodic necessity for replacement of the batteries that power the sensors. The system, which was equipped with wireless sensors, provided substantial amounts of research data during its operation.

The analysis of data collected during almost a year of research revealed significant changes in the technical condition of fan No. 2. A second-degree polynomial increase in vibration acceleration recorded by the S76 sensor was detected. This indicates the need for extended diagnostics and repair of this fan. Data from the following four weeks confirmed with high accuracy the forecast of changes in the fan's vibration level made by the developed $f_3(t)$ function.

The average weekly vibration acceleration values can be used as an indicator of vibration level changes. This parameter was calculated for a set of RMS values and shows a very high correlation coefficient square value of 0,997. In the case of vibration accelerations measured by the S76 sensor, the average weekly maximum values are closely correlated with the average weekly RMS values. It follows that, in theory, either of the two aforementioned data sets can be selected as the basis for assessing the technical condition of this machine. However, the recorded RMS values approximately twice as low, so they are more useful for diagnostics in the event of a significant increase in vibration. This can be seen in Figure 8, where the upper measurement range of the sensor is exceeded for the max. measurement series, while the RMS values are measured correctly.

During the 292 days of research, the vibration level of fan No. 1 underwent slight changes, which are visible in the weekly acceleration histograms. Based on the collected results, it was possible to select functions that reflect these changes. However, due to the fact that the average weekly effective values of vibration acceleration during the test period changed by only about 10%, the selected functions show a noticeably lower correlation with the test data than in the case of fan No. 2, due to the natural spread of the measurement results. It is

therefore necessary to continue research on this device and to conduct a subsequent re-analysis of a broader research material.

- **Source of funding:** This research received no external funding.
- Acknowledgment: The research data was obtained thanks to The Polish National Centre for Research and Development project no. POIR.01.01.01-00-0304/19-00, titled 'Hardware and software system for the diagnostics of machines and devices based on a wireless network of monitoring sensors and methods of knowledge engineering and computational intelligence'.
- **Author contributions:** research concept and design, Ł.D.; Collection and/or assembly of data, Ł.D.; Data analysis and interpretation, K.W.; Writing the article, K.W.; Critical revision of the article, K.W.; Final approval of the article, K.W.
- **Declaration of competing interest:** The authors declare that they have no known competing financial interests or personal relationships that could have appeared to influence the work reported in this paper.

REFERENCES

- Lei Y, Liu Z, Lin J, Lu F. Phenomenological models of vibration signals for condition monitoring and fault diagnosis of epicyclic gearboxes. Journal of Sound and Vibration. 2016;369:266-281. https://doi.org/10.1016/j.jsv.2016.01.016.
- Ruiz-Cárcel C, Jaramillo V.H, Mba D, Ottewill J.R, Cao Y. Combination of process and vibration data for improved condition monitoring of industrial systems working under variable operating conditions. Mechanical Systems and Signal Processing. 2016;66– 67:699-714.
 - https://doi.org/10.1016/j.ymssp.2015.05.018.
- Rabelo Baccarini L.M, Rocha e Silva V.V, Rodrigues de Menezes B, Matos Caminhas W. SVM practical industrial application for mechanical faults diagnostic Expert Systems with Applications 2011; 38(6): 6980-6984. https://doi.org/10.1016/j.eswa.2010.12.017.
- Fedorova D, Tlach V, Kuric I, Dodok T, Zajačko I, Tucki K. Technical diagnostics of industrial robots using vibration signals: Case study on detecting base unfastening. Applied Sciences. 2025;15(1):270. https://doi.org/10.3390/app15010270.
- Hassan IU, Panduru K, Walsh J. An in-depth study of vibration sensors for condition monitoring. Sensors. 2024;24(3):740. https://doi.org/10.3390/s24030740.
- Celiński I, Burdzik R, Młyńczak J, Kłaczyński M. Research on the applicability of vibration signals for real-time train and track condition monitoring. Sensors. 2022;22(6):2368. https://doi.org/10.3390/s22062368.
- Villarroel A, Zurita G, Velarde R. Development of a low-cost vibration measurement system for industrial applications. Machines. 2019;7(1):12. https://doi.org/10.3390/machines7010012.
- 8. Charles P, Sinha KJ, Gu F, Lidstone L, Ball A.D. Detecting the crankshaft torsional vibration of diesel engines for combustion related diagnosis. Journal of Sound and Vibration. 2009; 321(3–5): 1171-1185. https://doi.org/10.1016/j.jsv.2008.10.024.

- Burdzik R. A comprehensive diagnostic system for vehicle suspensions based on a neural classifier and wavelet resonance estimators. Measurement. 2022; 200:111602:1-17.
 - https://doi.org/10.1016/j.measurement.2022.111602.
- Burdzik R. Impact and assessment of suspension stiffness on vibration propagation into vehicle. Sensors. 2023;23(4):1930. https://doi.org/10.3390/s23041930.
- 11. Khan D, Burdzik R. Measurement and analysis of transport noise and vibration: A review of techniques, case studies, and future directions. Measurement. 2023;220:113354.
 - https://doi.org/10.1016/j.measurement.2023.113354.
- 12. Burdzik R. Application of vibration signals as independent and alternative information channels to support the reliability of positioning and prediction systems for transport means movement. Eksploatacja i Niezawodność Maintenance and Reliability. 2025;27(1). https://doi.org/10.17531/ein/196929.
- 13. Tiboni M, Remino C, Bussola R, Amici C. A review on vibration-based condition monitoring of rotating machinery. Applied Sciences. 2022;12(3):972. https://doi.org/10.3390/app12030972.
- Nguyen VH, Rutten C, Golinval JC. Fault diagnosis in industrial systems based on blind source separation techniques using one single vibration sensor. Shock and Vibration. 2012;19:183541 https://doi.org/10.3233/SAV-2012-0688.
- Hermansa M, Kozielski M, Michalak M, Szczyrba K, Wróbel Ł, Sikora M. Sensor-based predictive maintenance with reduction of false alarms – A case study in heavy industry. Sensors. 2022;22(1):226. https://doi.org/10.3390/s22010226.
- 16. Feng Z, Liang M. Complex signal analysis for wind turbine planetary gearbox fault diagnosis via iterative atomic decomposition thresholding. Journal of Sound and Vibration. 2014;333(20):5196-5211. https://doi.org/10.1016/j.jsv.2014.05.029.
- 17. Chu T, Nguyen T, Yoo H, Wang J. A review of vibration analysis and its applications. Heliyon. 2024; 10(5):12. https://doi.org/10.1016/j.heliyon.2024.e26282.
- Caesarendra W, Tjahjowidodo T. A Review of feature extraction methods in vibration-based condition monitoring and its application for degradation trend estimation of low-speed slew bearing. Machines. 2017; 5(4):21. https://doi.org/10.3390/machines5040021.
- Borecki M, Prus P, Korwin-Pawlowski M, Rychlik A, Kozubel W. Sensor set-up for wireless measurement of automotive rim and wheel parameters in laboratory conditions. Proc. SPIE. 2017;10445:1044569. https://doi.org/10.1117/12.2280970.
- Ma L, Li Z, Yang S, Wang J. A review on vibration sensor: key parameters, fundamental principles, and recent progress on industrial monitoring applications. Vibration. 2025;8(4):56. https://doi.org/10.3390/vibration8040056.
- Grega R, Czech P. Non-invasive vibroacoustic diagnostics of car internal combustion engines.
 Scientific Journal of Silesian University of Technology. Series Transport. 2024;125:69-87. https://doi.org/10.20858/sjsutst.2024.125.5.
- 22. Wojnar G, Burdzik R, Wieczorek AN, Konieczny Ł. Multidimensional data interpretation of vibration signals registered in different locations for system condition monitoring of a three-stage gear transmission operating under difficult conditions.

- Sensors. 2021;21(23):7808. https://doi.org/10.3390/s21237808.
- 23. Ghazali M, Hazwan M, Wan R. Vibration analysis for machine monitoring and diagnosis: A systematic review. Shock and Vibration. 2021;9469318:25. https://doi.org/10.1155/2021/9469318.
- 24. Vishwakarma M, Purohit R, Harshlata V, Rajput P. Vibration analysis & condition monitoring for rotating machines: A review. Materials Today: Proceedings. 2017;4(2):2659-2664. https://doi.org/10.1016/j.matpr.2017.02.140.
- 25. Su Z, Wang P, Yu X, Lv Z. Experimental investigation of vibration signal of an industrial tubular ball mill: Monitoring and diagnosing. Minerals Engineering. 2008;21:699-710. https://doi.org/10.1016/j.mineng.2008.01.009
- 26. Hermansa M, Sikora M, Sikora B, Wróbel Ł. Recommendation algorithm based on survival action Applied Sciences. 2024;14(7):2939. https://doi.org/10.3390/app14072939.
- 27. Cong F, Chen J, Dong G, Pecht M. Vibration model of rolling element bearings in a rotor-bearing system for fault diagnosis. Journal of Sound and Vibration. 2013;332(8):2081-2097. https://doi.org/10.1016/j.jsv.2012.11.029.
- 28. Wang X, Makis V, Yang M. A wavelet approach to fault diagnosis of a gearbox under varying load conditions. Journal of Sound and Vibration. 2010; 329(9):1570-1585. https://doi.org/10.1016/j.jsv.2009.11.010.
- 29. Sbarufatti C, Manson G, Worden K. A numericallyenhanced machine learning approach to damage diagnosis using a Lamb wave sensing network. Journal of Sound and Vibration. 2014; 333(19): 4499-4525. https://doi.org/10.1016/j.jsv.2014.04.059.
- 30. Tama B.A, Vania M, Lee S, Lim S. Recent advances in the application of deep learning for fault diagnosis of rotating machinery using vibration signals. Artificial Intelligence Review. 2023; 56: 4667-4709. https://doi.org/10.1007/s10462-022-10293-3.
- 31. Bhuiyan MR, Uddin J. Deep transfer learning models for industrial fault diagnosis using vibration and acoustic sensors data: A review. vibration. 2023;6(1): 218-238. https://doi.org/10.3390/vibration6010014.
- 32. Wang J, Hu H. Vibration-based fault diagnosis of pump using fuzzy technique. Measurement. 2006;
 - https://doi.org/10.1016/j.measurement.2005.07.015.
- 33. Burdzik R, Stanik Z, Warczek J. Method of assessing the impact of material properties on the propagation of vibrations excited with a single force impulse. Archives of Metallurgy and Materials. 2012;57(2): 409-416. https://doi.org/10.2478/v10172-012-0040-5.
- 34. Łuczak D, Brock S, Siembab K. Cloud based fault diagnosis by convolutional neural network as timefrequency rgb image recognition of industrial machine vibration with internet of things connectivity. Sensors. 2023;23(7):3755. https://doi.org/10.3390/s23073755.
- 35. Ragam P, Sahebraoji ND. Application of MEMSbased accelerometer wireless sensor systems for monitoring of blast-induced ground vibration and structural health: a review. IET Wireless Sensor Systems. 2019;9(3):103-109. https://doi.org/10.1049/iet-wss.2018.5099.
- 36. Rubes O, Chalupa J, Ksica F, Hadas Z. Development and experimental validation of self-powered wireless vibration sensor node using vibration energy harvester. Mechanical Systems and Signal Processing.

- 2021:160:107890. https://doi.org/10.1016/j.ymssp.2021.107890.
- 37. Juzek M, Słowiński P. The impact of accelerometer mounting on the correctness of the results obtained in ndt-type tests. Transport Problems. 2024;19(1):97-105. https://doi.org/10.20858/tp.2024.19.1.08.
- 38. Zhang X, Rane K, Kakaravada I, Shabaz M. Research on vibration monitoring and fault diagnosis of rotating machinery based on internet of things technology. 2021;10(1):245-254. Nonlinear Engineering. https://doi.org/10.1515/nleng-2021-0019.
- 39. Duss Ł, Sobczyk J. Measurement data from industrial fan vibration sensors. RepOD open database. 2025. https://doi.org/10.18150/QR053D.
- 40. Liu H, Zhang J, Cheng Y, Lu C. Fault diagnosis of gearbox using empirical mode decomposition and multi-fractal detrended cross-correlation analysis Journal of Sound and Vibration. 2016;385:350-371. https://doi.org/10.1016/j.jsv.2016.09.005.
- 41. Witaszek K, Witaszek M. Diagnosing the thermostat using vehicle on-board diagnostic (OBD) data. Diagnostyka. 2023;24(4):2023402. https://doi.org/10.29354/diag/173002.



Kazimierz WITASZEK received M.Sc. and PhD degrees in transport, from the University Silesian Technology (SUT). He works on the Faculty of Transport and Aviation Engineering. research is focused measurement, data processing, artificial neural networks, durability and reliability of

machine components especially in automotive sector. e-mail: kazimierz.witaszek@polsl.pl



Łukasz DUSS Received his B.Sc. degree in Computer Science with a specialization in Software Engineering from the University of Information Technology in Katowice. His professional activities focus on software development and DevOps methodologies. His research interests include data processing, data pipelines, and

the application of Generative Artificial Intelligence in intelligent information systems.

e-mail: l.duss@somar.com.pl